

Review

# Catechol-Based Antimicrobial Polymers

Seyedehfatemeh Razaviamri, Kan Wang, Bo Liu \* and Bruce P. Lee \* 

Department of Biomedical Engineering, Michigan Technological University, Houghton, MI 49931, USA; srazavia@mtu.edu (S.R.); kanwang@mtu.edu (K.W.)

\* Correspondence: bliu5@mtu.edu (B.L.); bplee@mtu.edu (B.P.L.)

**Abstract:** Catechol is a key constituent in mussel adhesive proteins and is responsible for strong adhesive property and crosslinking formation. Plant-based polyphenols are also capable of chemical interactions similar to those of catechol and are inherently antimicrobial. This review reports a series of catechol-based antimicrobial polymers classified according to their antimicrobial mechanisms. Catechol is utilized as a surface anchoring group for adhering monomers and polymers of known antimicrobial properties onto various types of surfaces. Additionally, catechol's ability to form strong complexes with metal ions and nanoparticles was utilized to sequester these antimicrobial agents into coatings and polymer matrices. During catechol oxidation, reactive oxygen species (ROS) is generated as a byproduct, and the use of the generated ROS for antimicrobial applications was also introduced. Finally, polymers that utilized the innate antimicrobial property of halogenated catechols and polyphenols were reviewed.

**Keywords:** catechol; polymer; antimicrobial; reactive oxygen species



**Citation:** Razaviamri, S.; Wang, K.; Liu, B.; Lee, B.P. Catechol-Based Antimicrobial Polymers. *Molecules* **2021**, *26*, 559. <https://doi.org/10.3390/molecules26030559>

Academic Editor:

Matthias Schnabelrauch

Received: 24 December 2020

Accepted: 19 January 2021

Published: 21 January 2021

**Publisher's Note:** MDPI stays neutral with regard to jurisdictional claims in published maps and institutional affiliations.



**Copyright:** © 2021 by the authors. Licensee MDPI, Basel, Switzerland. This article is an open access article distributed under the terms and conditions of the Creative Commons Attribution (CC BY) license (<https://creativecommons.org/licenses/by/4.0/>).

## 1. Introduction

Infection associated with microorganisms such as bacteria, viruses, fungi, or parasites results in more death worldwide when compared with other causes [1,2]. To date, there are many different strategies to prevent bacterial growth and infection. The most widely used antimicrobial strategy is the use of small antimicrobial molecules that are broadly applied such as antibiotics, antiseptics, disinfectants, and preservatives. However, overreliance on the use of these compounds has resulted in the formation of drug-resistant microorganisms due to their ability to rapidly mutate [3,4]. For instance, *Pseudomonas aeruginosa* and *Staphylococcus aureus* are resistant to many antibiotics [5].

Challenged by the ongoing threats from antibiotic-resistant microorganisms, polymers with intrinsic antimicrobial properties have received increased interest in both the academia and the industry [6,7]. Antimicrobial polymers are either functionalized with antimicrobial agents [8] or possess innate antimicrobial properties [9–11]. There are several categories of antimicrobial polymers, which include cationic polymers [12,13], polymers that mimic natural peptides [14–17], halogenated polymers [15,18], and polymers containing metal ions or nanoparticles (NPs) [19]. Antimicrobial polymers can slow or inhibit the growth of drug-resistant strains [9,10] and present high antimicrobial efficacy due to the various antimicrobial modes and polymeric structures [4]. Additionally, these antimicrobial polymers are promising materials with less toxicity to the human body, long-lasting activity, and higher environmental safety than the traditional disinfectants [20,21].

Catechol and polyphenols are widely found in nature. Marine mussels secrete adhesive proteins that consist of a large abundance of 3,4-dihydroxyphenyl-L-alanine (DOPA), an amino acid with a catechol side chain [22–24]. The presence of catechol contributes to both the interfacial binding and curing of these adhesive proteins [25]. Catechol can participate in a wide range of reversible interactions (e.g., hydrogen bonding,  $\pi$ - $\pi$  electron interaction, cation- $\pi$  interaction, coordination with metal oxide surfaces and metal ions), and covalent bond formation (Figure 1) [23]. Incorporating catechol into the polymers

imparts these materials with the chemical reactivity of catechol for designing adhesives, antifouling coatings, drug carriers, and antimicrobial polymers [26–30]. Similarly, plant-based polyphenols such as tannic acid (TA) and catechin exhibit intermolecular interactions and crosslinking capability resembling those of catechol [31–33]. While most scientists utilize these compounds predominantly as a surface anchoring group for promoting interfacial bonding, recent research indicated that catechol generates reactive oxygen species (ROS) as a byproduct during catechol oxidation [34]. ROS has been demonstrated to function as an effective, broad-spectrum biocide in many industrial and biomedical applications [35,36]. Additionally, catechol chemically modified with a halogen [37] and polyphenols such as TA, curcumin, catechin, and procyanidin [38–40] are innately antimicrobial.

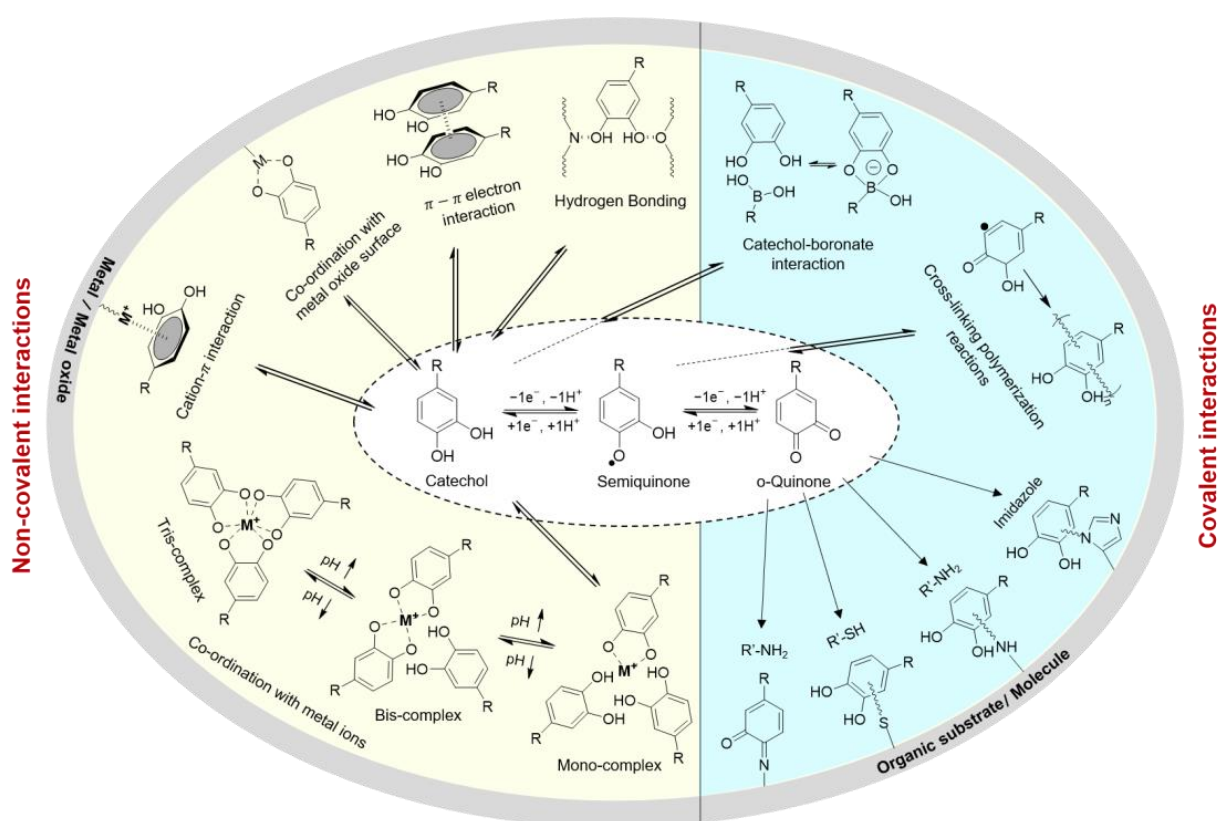


**Figure 1.** Possible interactions and reactions of catechol, semiquinone, and ortho-quinones. Noncovalent interactions include hydrogen bonding,  $\pi$ - $\pi$  electron interaction, coordination with metal oxide surface, cation- $\pi$  interaction, and coordination with metal ions. Covalent interactions include catechol-boronate complexation, polymerization, and irreversible bonding to organic substrates or molecules bearing, -thiol, -amine, and -imidazole functional groups.

This review focuses on catechol-based antimicrobial polymers. First, the use of catechol moieties as a surface anchoring group to immobilize antimicrobial polymers is reviewed. Then, the use of catechol-modified polymers to sequester metal ions or NPs is introduced. Next, the ability for catechol to generate antimicrobial levels of ROS is introduced. Finally, the antimicrobial activity of halogenated catechol and polyphenols is reviewed.

## 2. Catechol-Modified Polymers with Innate Antimicrobial Properties

Catechol can be incorporated into polymer chains by copolymerizing catechol-containing monomers with plant-based antimicrobial monomers or cationic monomers to prepare robust and biocompatible antimicrobial polymers and coatings [26,41]. Alternatively, catechol can be tethered to cationic polymers with known antimicrobial properties to

synthesize antimicrobial polymers. In this strategy, catechol serves as the surface anchoring group to adhere these antimicrobial polymers onto various types of surfaces.

Monomers with cardanol side chains, 2-hydroxy-3-cardanylpropyl methacrylate (HCPM), were copolymerized with dopamine methacrylamide (DMA) to prepare an antimicrobial polymer, P(DMA-*co*-HCPM) (Figure 2a) [40]. Cardanol can be obtained from cashew nut shell liquid and has previously demonstrated antimicrobial property [42,43]. The P(DMA-*co*-HCPM)-coated polysulfone membranes exhibited excellent antibacterial activities against *Escherichia coli* and *S. aureus*, demonstrating a higher than 90% killing efficiency. Similarly, borneol is a natural plant-based antibiotic [44], and borneol-containing polymers demonstrated excellent antibacterial activities [45]. However, these polymers do not have a surface anchoring moiety to form stable coatings [46]. Block copolymers of poly(DMA) and poly (borneolacrylate) (P(DMA-*b*-BA)) (Figure 2b) demonstrated remarkable and long-lasting antibacterial properties against *E. coli* and *S. aureus* [47]. P(DMA-*b*-BA) coatings showed robust adhesion and bactericidal properties on different surfaces such as silicon, silica, stainless steel (SS), cotton fabric, commercial gauze, and alumina.

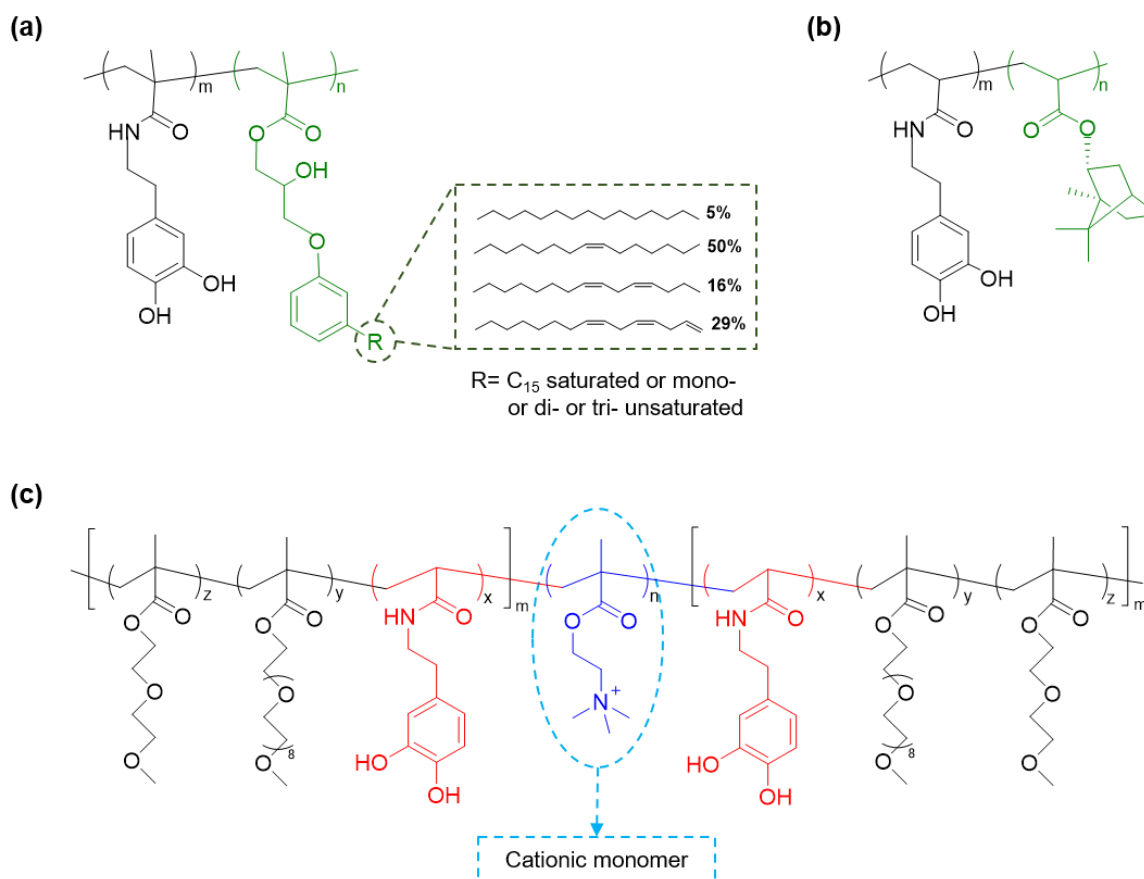


**Figure 2.** Chemical structures of polymers functionalized with catechol-based and antimicrobial monomers (a) P(DMA-*co*-HCPM), (b) P(DMA-*b*-BA), and (c) P(MEO<sub>2</sub>MA-*co*-OEGMA-*co*-DAA)-*b*-PMETA-*b*-P(MEO<sub>2</sub>MA-*co*-OEGMA-*co*-DAA).

Cationic polymers can kill pathogens by attacking their negatively charged cell walls and exhibit excellent antimicrobial properties [12]. The cationic monomer 2-(methacryloyloxy)ethyl trimethylammonium iodide (META) was copolymerized with polyethylene glycol (PEG) and catechol-based monomers to create a triblock copolymer poly{[2-(2-methoxyethoxy)ethyl methacrylate]-*co*-[oligo(ethylene glycol) methacrylate]-*co*-(*N*-3,4-dihydroxyphenethyl acrylamide)}-*b*-poly{[2-(methacryloyloxy)ethyl] trimethylammonium iodide}-*b*-poly{[2-(2-methoxyethoxy)ethyl methacrylate]-*co*-[oligo(ethylene glycol) methacrylate]-*co*-(*N*-3,4-dihydroxyphenethyl acrylamide)} (P(MEO<sub>2</sub>MA-*co*-OEGMA-*co*-DAA)-*b*-PMETA-*b*-P(MEO<sub>2</sub>MA-*co*-OEGMA-*co*-DAA)) (Figure 2c) [48]. This triblock copolymer can self-assemble to form

a self-healing hydrogel, while effectively suppressing the growth of *E. coli* owing to the presence of cationic quaternary ammonium salt. Additionally, the incorporation of antifouling PEG prevented nonspecific cell attachment. Similarly, catechol was copolymerized with 2-(4-methylthiazol-5-yl) ethyl methacrylate (MTA) [49] and 2-(dimethylamino)ethyl methacrylate (DMAEMA) [50] to create cationic antimicrobial polymers.

Qiu et al. [51] showed that through the co-deposition of catechol and cationic polyethylenimine (PEI), *N*-alkylated PEI was grafted onto polypropylene microfiltration membranes (PPMs) at pH 8.5. Catechols are oxidized into quinone states in a weak alkaline condition, subsequently reacting with amino groups of PEI via Michael addition or Schiff base reaction. The modified membrane surface demonstrated 95% antibacterial efficiency against *S. aureus* and weak adherence of bacterial cells after 24 h of incubation.

### 3. Catechol-Based Polymers in Combination with Metal Ions and Nanoparticles

Metal ions such as silver, copper, zinc, gold, and titanium can kill bacteria by binding to cell membrane proteins, thus inhibiting vital enzymatic activities for cell growth and causing metabolic disruption that leads to cell death [52,53]. Catechol can form reversible complexes with these metal ions in a pH-dependent manner [54,55]. Additionally, catechol can reduce soluble metal ions to form NPs, thus functionalizing the NPs on the surface of the catechol-containing polymer [56–58]. This section reviews catechol-containing polymers that contained various metal ions and NPs. In these polymer systems, catechol functions as an adhesive moiety for surface bonding as well as sequestering the antimicrobial metal ions and NPs.

#### 3.1. Silver Ions ( $Ag^+$ ) and Silver Nanoparticles (AgNPs)

Silver and its compounds are the most used metal ions in creating antimicrobial polymers [5]. When silver is ionized in solution, the bactericidal active  $Ag^+$  binds to the proteins of cell walls and form complexes with the DNA and RNA of bacteria, leading to broad-spectrum antimicrobial activity [59,60].  $Ag^+$  and AgNPs can be incorporated into copolymers, hydrogels, or coatings to create antimicrobial polymeric materials [30,61]. Catechol-containing polymers have been demonstrated to reduce water-soluble  $Ag^+$  to form AgNPs (Figure 3), effectively encapsulating the AgNPs into the polymer matrices. In this approach, catechol not only serves as the reducing agent but also stabilizes the in situ formed AgNPs. Huang et al. [62] prepared catechol-modified chitosan (Figure 4a), which reduced  $Ag^+$  in the form of silver nitrate ( $AgNO_3$ ) in solution to form an antimicrobial chitosan/AgNP composite. This composite exhibited remarkable antimicrobial performance at a very low dosage, with a minimum bactericidal concentration of  $14 \mu g \cdot mL^{-1}$  against *E. coli* and  $25 \mu g \cdot mL^{-1}$  against *S. aureus*. In another approach, O-carboxymethyl chitosan (CMC) was directly reacted with catechol and deposited onto polyethersulfone (PES) membranes to construct a coating loaded with AgNPs [63]. Carboxyl and amino groups in CMC captured  $Ag^+$ , which was reduced to AgNPs by catechol moieties. Then PEG-based polyurethane (PU) was added to confer antifouling properties to the membrane. The chitosan/AgNP and CMC-Ag-PU composites can be deposited onto titanium and PES surfaces, respectively, by utilizing the strong adhesive and redox property of catechol [63,64]. Both surfaces exhibited strong antibacterial and antifouling properties against *E. coli* and *S. aureus*. Similarly, a copolymer with a cationic methacrylate bearing a quaternary ammonium group, 2-methacryloxyethyltrimethylammonium chloride (DMAEMA<sup>+</sup>), and a methacrylamide bearing DOPA group (poly(mDOPA)-*co*-poly(DMAEMA<sup>+</sup>)) (Figure 4b) was applied to fabricate an antimicrobial coating for SS [65]. This cationic polymer in combination with a polyanion, poly(styrene sulfonate), was deposited on the SS surface by electrostatic interaction. Both DOPA and poly(DMAEMA<sup>+</sup>) formed and stabilized bactericidal AgNPs. This coating showed excellent killing capability against *E. coli*. The antimicrobial  $Ag^+$  can be reloaded to replenish the antimicrobial coating. This approach utilized a one-pot preparation, which is more convenient than the layer by layer (LbL) deposition in which 45–60 bilayers are needed to have a comparable antimicrobial activity [66].

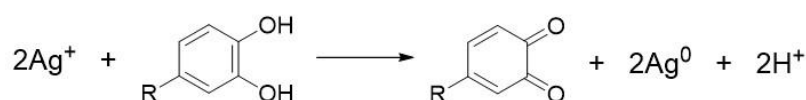


**Figure 3.** Silver nanoparticle (AgNP) preparation through the reduction of  $\text{Ag}^+$  by catechol as a reducing agent.

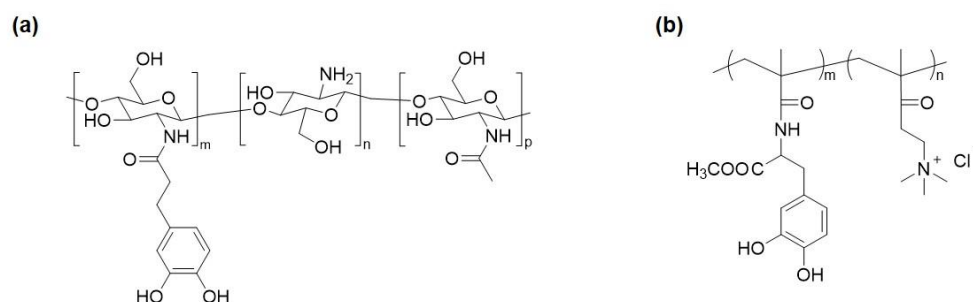


**Figure 4.** (a) Catechol-modified chitosan and (b) poly(mDOPA)-co-poly(DMAEMA<sup>+</sup>).

In addition to the catechol-based copolymers, diverse antimicrobial catechol-based hydrogels containing AgNPs were also reported. Le Thi et al. [67] described catechol-functionalized gelatin hydrogels loaded with AgNPs for enhanced antimicrobial activities. This composite hydrogel sustainably released  $\text{Ag}^+$  over a period of 14 days, which demonstrated the ability to inhibit the growth of both *E. coli* and *S. aureus* bacteria. Similarly, GhavamiNejad et al. [68] embedded AgNPs into a zwitterionic hydrogel copolymerized with DMA. This composite hydrogel exhibited strong antibacterial properties against Gram-negative (*E. coli*) and Gram-positive (*S. aureus* and *P. aeruginosa*) bacteria. Other monomers such as non-ionic, cationic, and anionic monomers can be used instead of zwitterionic monomers to fabricate AgNP-containing nanocomposite hydrogels.

There are limitations for using AgNPs in biomedical applications due to its potential for causing mammalian cell apoptosis and death [69,70]. Dopamine-conjugated polymers can be used to reduce the toxicity of AgNPs toward mammalian cells [71]. In this one-step approach, antimicrobial and biocompatible catechol-containing silver-carbon nanotube composites (AgNP-CNT) were produced. A catechol-containing heparin-mimetic polymer was used to convert  $\text{Ag}^+$  to AgNPs and anchor them onto the surface of the CNT composites. The composite coatings demonstrated a great antibacterial activity against *E. coli* and *S. aureus* with the killing efficiency of 77.3% and 81.2%, respectively. Interestingly, the shielding effects of the catecholic polymer coating and the bioactivity of the heparin-like polymer resulted in the improvement of the cytocompatibility of the antimicrobial nanocomposites and inhibited the direct cellular exposure to AgNPs.

Gan et al. [72] developed a plant-based hydrogel containing Ag-lignin NPs, pectin (P), and poly acrylic acid (PAA). Lignin possesses the reductive phenolic hydroxyl and methoxy groups, which can reduce  $\text{Ag}^+$  to AgNPs. The Ag-lignin NPs-P-PAA hydrogel displayed long-term adhesion, high toughness, and strong antimicrobial properties. The increased adhesive property was due to the continuous generation of the catechol from of lignin through a balanced redox reaction inside the hydrogel network. This hydrogel effectively inhibited *E. coli* (97%) and *Staphylococcus epidermidis* (98%). The antibacterial activities of NPs-P-PPA in vivo were confirmed in a rabbit model following the injection of *E. coli* suspension ( $1 \text{ mL}, 10^5 \text{ cells mL}^{-1}$ ).

### 3.2. Other Metal Ions and Nanoparticles

Iron ion ( $\text{Fe}^{3+}$ ) is widely found in mussel byssus along with catechol-containing proteins [73]. The catechol- $\text{Fe}^{3+}$  interaction has been reported as a tool for developing an antimicrobial polymer film on a solid surface [74]. Alginate-functionalized with catechol (Alg-C) was deposited onto polydopamine (PDA)-coated substrate and  $\text{Fe}^{3+}$  was introduced as the crosslinker to construct a multilayered film (Figure 5). PDA was first described

by the Messersmith lab [75] and is a facile method to form multifunctional coatings consisting of polymerized form of dopamine. The Alg-C/Fe<sup>3+</sup> multilayered films prevented bacterial adhesion and films with a thickness greater than 10 nm demonstrated the ability to inhibit bacterial growth for over 24 h.

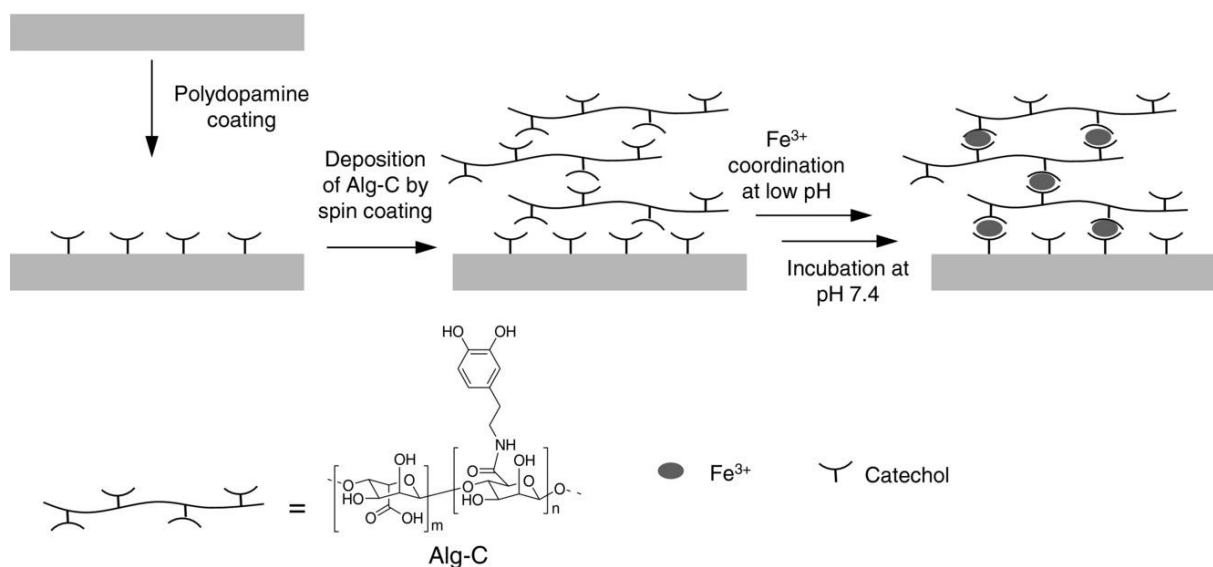


**Figure 5.** Alg-C/Fe<sup>3+</sup> coating. Catechol-Fe<sup>3+</sup>-catechol interactions are the bridge to construct the antimicrobial multilayer film. Reprinted with permission from reference [74], copyright 2016 Wiley.

Siderophores are iron-chelating compounds, secreted by cells to gather iron from external sources [76]. Artificial catechol-containing siderophores conjugated with antimicrobial drugs displayed potent antimicrobial activity against multidrug-resistant bacteria. These catecholate siderophores form complex with Fe<sup>3+</sup> and enter the microorganism via the corresponding siderophore-uptake pathway to deliver the antimicrobial drug to the bacterial cell. These drug conjugates exhibited strong antibacterial activities against Gram-negative bacteria such as *P. aeruginosa*, which is highly resistant to most of the existing antibiotics [77]. Some conjugates exhibited a minimum inhibitory concentration lower than 0.25 µg·mL<sup>-1</sup> when treated against aminopenicillin-resistant strains [78].

Molybdenum trioxide (MoO<sub>3</sub>) NPs also demonstrated strong antimicrobial activity [56,57]. However, the application of MoO<sub>3</sub> NPs is limited by their poor solubility in water. Catechol-containing polymers such as poly(dopamine methacrylamide-co-methoxyethyl acrylate), poly(dopamine methacrylamide), poly(ethyl methacrylate-co-dopamine methacrylamide), and poly(hydroxyethyl methacrylate-co-dopamine methacrylamide) were used to secure MoO<sub>3</sub> NPs on surfaces [58]. These nanocomposite coatings not only killed *E. coli* and *Bacillus subtilis* after only 1 h of incubation, but they were also antimicrobial against the more antibiotic-resistant Gram-negative (*P. aeruginosa*) and Gram-positive (*Streptococcus pyogenes* and *S. epidermidis*) bacteria strains after 2 h of incubation. These coatings also demonstrated the ability to inhibit the growth of biofilms.

#### 4. ROS-Releasing Catechol-Based Polymers

ROS are highly reactive molecules and free radicals derived from molecular oxygen [79]. ROS can degrade organic compounds [80–82], initiate free radical polymerization [83], and kill cells [84,85]. ROS kills cells by attacking and destroying proteins, lipids, and DNA, which makes ROS a potential solution for antimicrobial applications [86]. Catechol generates various types of ROS such as hydrogen peroxide (H<sub>2</sub>O<sub>2</sub>), superoxide (O<sub>2</sub><sup>-</sup>), singlet oxygen (<sup>1</sup>O<sub>2</sub>), and hydroxyl radical (•OH) during oxidizing conditions such as autoxidation [34], chemical-induced oxidation [87], and metal ion-mediated oxidation [87,88].

$\text{H}_2\text{O}_2$  is generated as a byproduct during the autoxidation of catechol at a neutral to basic pH (Figure 6a) [34]. Catechol-modified microgels generated 1–5 mM of  $\text{H}_2\text{O}_2$  over a period of 4 days as catechol autoxidized through simple hydration [28]. The  $\text{H}_2\text{O}_2$  generated from these microgels completely prevented colony formation of both Gram-negative (*E. coli*) and Gram-positive (*S. epidermidis*) bacteria within 24 h and inactivated the infectivity of both enveloped bovine viral diarrhea virus (BVDV) and non-enveloped porcine parvovirus (PPV). By controlling the oxidation state of catechol, these microgels can be repeatedly activated (pH 7.4) and deactivated (pH 3.5) to generate antipathogenic levels of  $\text{H}_2\text{O}_2$ . These microgels do not contain the reactive ROS, and  $\text{H}_2\text{O}_2$  is generated by converting molecular oxygen in the aqueous solution through catechol oxidation. This simple activation process enables the catechol-modified microgel to function as a lightweight and portable source of disinfectant.

$\text{H}_2\text{O}_2$  is not a very potent disinfectant and bacteria such as *Staphylococcus* secrete antioxidant enzymes such as catalase that decomposes  $\text{H}_2\text{O}_2$  [89]. To further enhance the antimicrobial property of catechol-modified microgels, these microgels were further chemically modified with hematin (HEM), a porphyrin derivative that contains an  $\text{Fe}^{3+}$  ion (Figure 6b) [90].  $\text{Fe}^{3+}$  can convert the generated  $\text{H}_2\text{O}_2$  to  $\bullet\text{OH}$  via a Fenton-like reaction process.  $\bullet\text{OH}$  is also a highly reactive and strong oxidant with remarkable antimicrobial properties [91]. These microgels demonstrated faster and more effective antibacterial activities against both Gram-negative (*E. coli*) and Gram-positive (*S. epidermidis*) bacteria at concentrations of  $10^6$  and  $10^7$  CFU·mL<sup>-1</sup>, when compared to microgels that generated only  $\text{H}_2\text{O}_2$  [90]. These microgels also reduced 99.997% and 99.97% infectivity of BVDV and PPV, respectively. However,  $\bullet\text{OH}$  alone did not provide sufficient antimicrobial property due to its short half-life ( $10^{-9}$  s) [92]. To overcome this issue, the microgels were further modified with positively charged [2-(methacryloyloxy)ethyl] trimethylammonium chloride (METAC), which enhances the antibacterial performance of the microgel through electrostatic interactions between the positively charged microgels and the negatively charged pathogens [90].

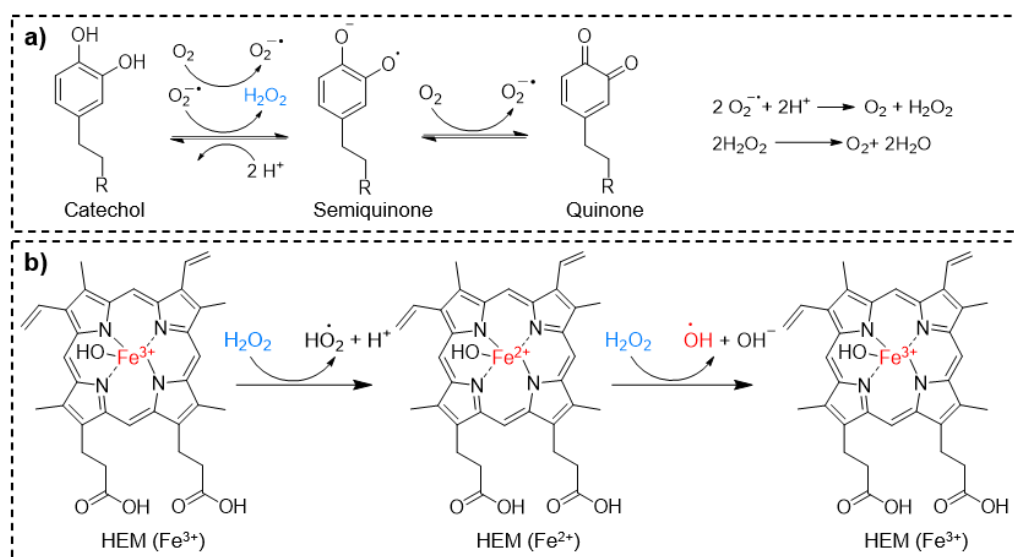


**Figure 6.** Schematics showing the mechanism of catechol oxidation and  $\text{H}_2\text{O}_2$  generation (a) and  $\text{H}_2\text{O}_2$  decomposition to generate  $\bullet\text{OH}$  in the presence hematin (HEM) (b). Reproduced with permission from reference [90] copyright 2020 American Chemical Society.

Catechol generates  $\text{O}_2^{\bullet-}$  in metal ion-mediated oxidation, which can be further converted into  $^1\text{O}_2$  by the metal ion [88,93]. Both  $\text{O}_2^{\bullet-}$  and  $^1\text{O}_2$  are more reactive when compared to  $\text{H}_2\text{O}_2$ . When catechol-modified microgels were incubated in solutions containing up to 40 mM of various metal ions (e.g.,  $\text{Fe}^{2+}$ ,  $\text{Ni}^{2+}$ ,  $\text{Cu}^{2+}$ ,  $\text{Co}^{2+}$ ) more than 85% of

these metal ions were removed from the solution [88]. Most interestingly, these metal ions were repurposed to generate ROS for dye degradation. Similarly,  $^1\text{O}_2$  was produced by oxidizing catechol-modified microgel with iron magnetic nanoparticles (FeMNPs) instead of metal ions (Figure 7). Unlike autoxidation of catechol that occurs only at a basic pH, the ROS generation occurred over a wide range of pH (pH 3 to 9). The generated  $^1\text{O}_2$  killed 99% of *E. coli* after 24 h of incubation, degraded organic dyes, and removed the antibiotic ciprofloxacin from the solution. This simple mixture of catechol-modified microgel and FeMNPs can potentially be utilized as a portable source for on-demand generation of ROS for bioremediation and water purification.

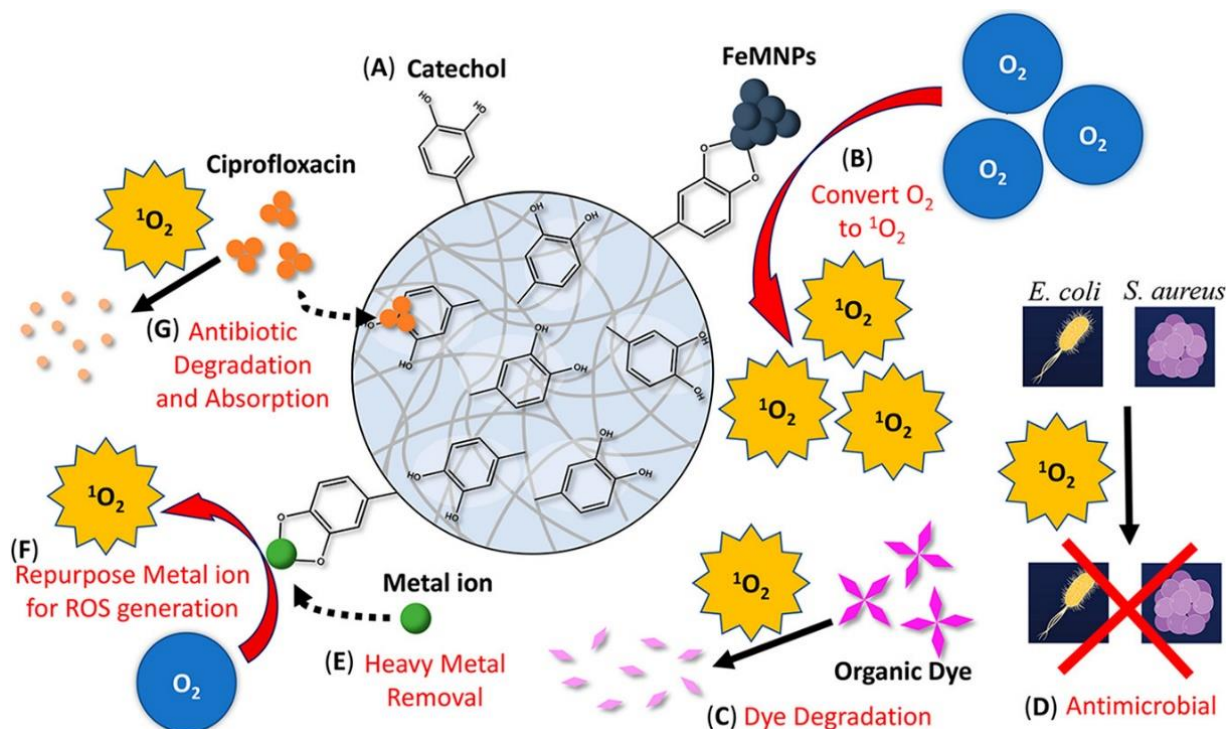


**Figure 7.** Multifunctional catechol-based microgel. Reprinted with permission from reference [88], copyright 2020 American Chemical Society.

Catechols in PDA coating also demonstrated the ability to generate  $\text{H}_2\text{O}_2$  [29]. However, to generate antimicrobial levels of  $\text{H}_2\text{O}_2$ , a two-step coating approach combined with gentle shaking was necessary (Figure 8). In the first coating step, a thick primer layer of PDA was coated onto the surface of polypropylene (PP) mesh utilizing an elevated level of dopamine ( $20 \text{ mg}\cdot\text{mL}^{-1}$ ). In the second step, a significantly lower concentration of dopamine ( $2 \text{ mg}\cdot\text{mL}^{-1}$ ) was applied for the formation and deposition of macroaggregates of PDA NPs formed in the solution. Shaking the solution during coating promoted gas exchange to increase molecular oxygen content in the reaction solution, which promoted catechol oxidation in creating a thicker PDA film. When the PDA-coated PP mesh was hydrated in a solution at pH 7.4,  $200 \mu\text{M}$  of  $\text{H}_2\text{O}_2$  was generated for over 48 h. The released  $\text{H}_2\text{O}_2$  completely killed *E. coli* and reduced the log reduction value of *S. epidermidis* by 98.9% within 24 h. Furthermore, PDA was coated on to SS to reduce adhesion of *Psychrobacter cryohalolentis* [94].



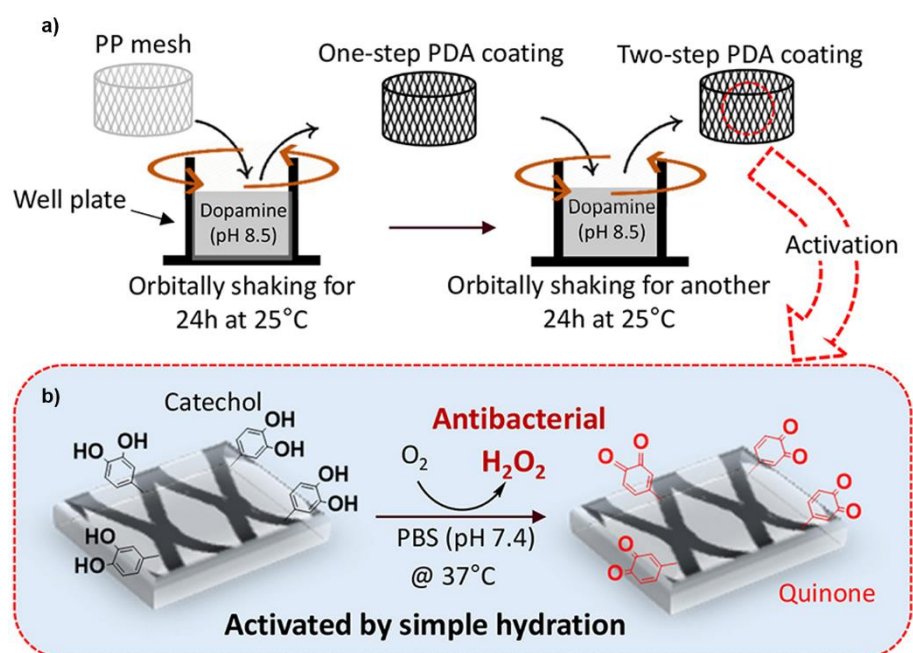


**Figure 8.** Schematic illustration of (a) catechol-based polydopamine (PDA) coating prepared by two-steps with gentle shaking and (b) the activation of the PDA-coated mesh to generate H<sub>2</sub>O<sub>2</sub> by simply hydrating the mesh in the PBS with at pH 7.4. Reprinted with the permission of reference [29], copyright 2019 Kord Forooshani et al.

## 5. Innate Antimicrobial Property of Halogenated Catechol and Polyphenols

### 5.1. Antimicrobial Halogenated Catechol

Halogenated phenols, such as triclosan and hexachlorophenol, can rupture and kill bacteria by deforming their cell walls, inhibiting their growth, and causing cytological damage [95]. Triclosan binds tightly to enoyl-acyl carrier protein reductase in complex with oxidized nicotinamide adenine dinucleotide (FadI/NAD<sup>+</sup>) to inhibit the synthesis of bacterial fatty acids and achieve a broad-spectrum antimicrobial effect [96,97]. The antimicrobial halogenated catechol also exists in nature. DOPA with a chloride-functionalized catechol side chain (Cl-DOPA) was extracted from a marine polychaete, *Phragmatopoma californica* [98]. PEG hydrogel chemically crosslinked using Cl-functionalized dopamine prevented *E. coli* adhesion rate by 20% [99].

Recently, our group prepared a series of DMA derivatives (chlorodopamine methacrylamide (DMA-Cl), bromodopamine methacrylamide (DMA-Br), and iododopamine methacrylamide (DMA-I)) modified with electron-withdrawing halogen substituents at the 6-position (Figure 9) [37]. These halogenated DMAs were incorporated into hydrogels, copolymers, and coatings through free-radical polymerization. The killing efficiency of halogenated DMA-containing polymers exhibited a 7 log reduction against *E. coli* and *S. aureus*. Most notably, DMA-Cl containing hydrogels effectively killed five multidrug-resistant (MDR) bacteria (methicillin-resistant *S. aureus*, vancomycin-resistant enterococci, multi-antibiotics-resistant *P. aeruginosa*, multi-antibiotics-resistant *Acinetobacter baumannii*, and carbapenem-resistant *Klebsiella pneumoniae*). All MDR bacteria were completely eradicated after 24 h of incubation. Additionally, these hydrogels also demonstrated the ability to kill bacteria in a biofilm while exhibiting low cytotoxicity. Interestingly, when the catechol side chain was protected with methoxy groups and rendered non-adhesive, the methoxy-protected catechol lost its antimicrobial activity. This indicated that the ability for catechol to adhere to the bacteria is critical for contact killing, which resulted in membrane disruption. Other halogenated catechol-based polymers such as chlorinated PDA (Cl-PDA) demonstrated a 5 log reduction in bacterial population against both *E. coli* and *S. aureus* [100].

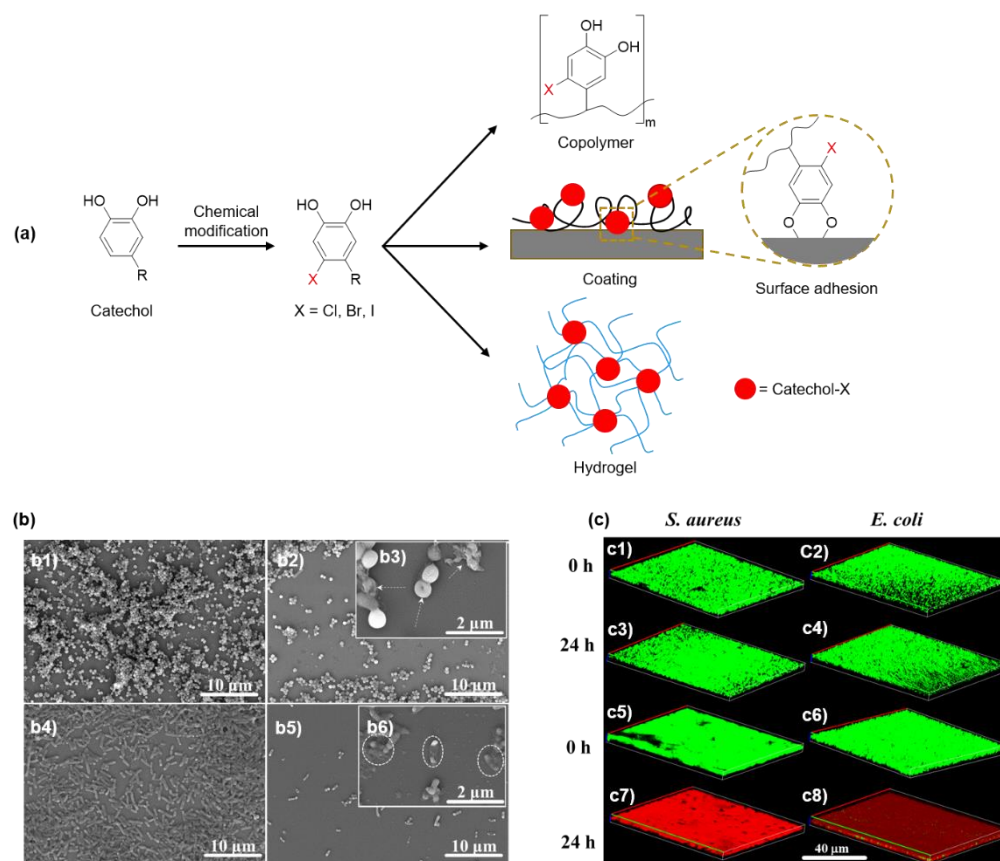


**Figure 9.** (a) Chemical structures of halogenated catechol, which was incorporated into copolymers, coatings, and hydrogels with antimicrobial property. (b) FE-SEM images of (b1) *S. aureus* grown after 24 h. (b2 and b3) *S. aureus* treated with DMA-Cl containing hydrogel for 24 h with the inset image showing magnified image of ruptured *S. aureus* and bacterial debris (white arrows). (b4) *E. coli* culture for 24 h. (b5 and b6) *E. coli* treated with DMA-Cl containing hydrogel for 24 h with the inset image showing magnified image of ruptured *E. coli* and bacterial debris (white circles). (c) Fluorescence images of LIVE/DEAD bacterial staining assay of *S. aureus* (c1 and c3) treated with catechol-free hydrogel and (c5 and c7) DMA-Cl-containing hydrogel after 0 and 24 h. Fluorescence images of LIVE/DEAD bacterial staining assay of *E. coli* (c2 and c4) treated with catechol-free hydrogel and (c6 and c8) DMA-Cl-containing hydrogel after 0 and 24 h. Live and dead cells are stained green and red, respectively. Reprinted from [37], copyright 2021, with permission from Elsevier.

## 5.2. Antimicrobial Polyphenols

Polyphenols such as TA, curcumin, catechin, and procyanidin (Figure 10) exhibit innate antimicrobial properties due to the abundant phenolic hydroxyl groups, which can denature bacterial proteins and damage bacterial cell membranes [38–40]. TA has demonstrated antimicrobial effect on *S. aureus* [101]. The antibacterial activity of TA largely relies on the content of phenolic hydroxyl groups [102]. Sahiner et al. [103] prepared a crosslinked poly(TA) hydrogel. Under acidic conditions (pH 5.4), p(TA) hydrolyzed into gallic acid, the minimum inhibition concentration (MIC) value of p(TA) against *S. aureus* was  $40 \mu\text{L}\cdot\text{mL}^{-1}$ . Under alkaline conditions (pH 9.0), p(TA) hydrolyzed and released TA, the MIC value of p(TA) against *S. aureus* was  $10 \mu\text{L}\cdot\text{mL}^{-1}$ . Li and coworkers [104] prepared hemostatic microparticles by crosslinking TA, carboxymethyl chitosan, hyaluronic acid, and starch. When this composite material was added to the wound site, it promoted rapid hemostasis, and the released TA exhibited antimicrobial effects against both *E. coli* and *S. aureus*. A series of UV-curable antibacterial resins were synthesized by modifying TA with different amounts of glycidyl methacrylate (GMA) [105]. This resin achieved diameters of zone of inhibition as high as 19 mm against *E. coli* and *S. aureus*. However,

with an elevated amount of GMA used to crosslink the resin, the resin lost antimicrobial property, indicating that the phenolic hydroxyl groups in TA played an important role in antibacterial activity [106].

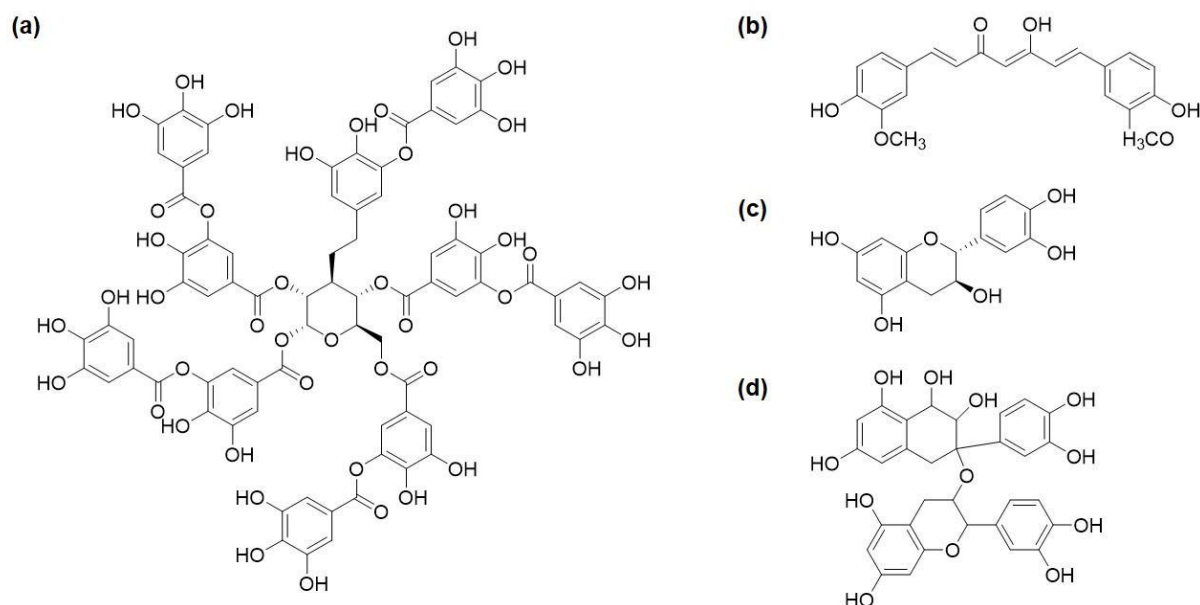


**Figure 10.** Chemical structures of antimicrobial polyphenols such as (a) TA, (b) curcumin, (c) catechin, and (d) procyanidin.

Other natural polyphenols such as tea catechins, curcumin from *Curcuma longa*, and procyanidins from grape seeds exhibit anti-tumor, anti-inflammatory, antioxidant, anti-obesity, and antimicrobial properties [107–112]. For example, theaflavin digallate (TFDG), a poly-catechin, can directly inhibit cytoplasmic membrane proteins to achieve an antimicrobial effect [113]. The membrane glucose transporters' activity decreased 40% after treatment with  $62.5 \text{ mg} \cdot \text{L}^{-1}$  TFDG. Similarly, nanofibrous membranes constructed from curcumin-containing polymer demonstrated to be effective antimicrobial barriers with antimicrobial activity that lasted over 7 days [111]. Procyanidins can serve as an antimicrobial drug [114]. Procyanidins were loaded into sugarcane bagasse hydrogel and exhibited antibacterial effect against *S. aureus*. Finally, procyanidin-treated crepe de Chine silk showed excellent flame-retardant and antimicrobial properties [115]. The treated silk maintains more than 80% antimicrobial activity after repeated washing for more than 20 times.

## 6. Summary and Future Outlooks

The use of antimicrobial polymers has been extended to many different fields due to their improved quality and safety in comparison to traditionally used biocides. This article reviewed different strategies to create antimicrobial polymers utilizing catechol chemistry. The adhesive property of catechol was utilized to anchor antimicrobial polymers to impart surfaces with antimicrobial property. Additionally, the ability for catechol to bind to metal ions and reduce metal nanoparticles was utilized to sequester these antimicrobial ions and particles into coatings and polymer matrices. ROS is a broad-spectrum disinfectant and is generated as a byproduct during catechol oxidation. The process of inducing in situ catechol oxidation is a recent strategy utilized to create portable biomaterials with the ability for on-demand generation of ROS for antimicrobial application. Finally, halogenated catechols and natural polyphenols exhibit innate antimicrobial property.

While catechol and catechol-containing biomaterials have proven to be biocompatible in culture and in preclinical studies [116–119], cytotoxic compounds are incorporated in designing antimicrobial polymers.  $\text{Ag}^+$  can interfere with mammalian cell function through a competitive protein complexation and silver-containing polymers can damage mammalian cells [69,70]. Antimicrobial metal oxides such as zinc and titanium with

improved biocompatibility can potentially be used instead of the cytotoxic  $\text{Ag}^+$  [120–122]. Similarly, halogenated catechol such as chlorocatechols had been demonstrated to be toxic to zebra fish, a model organism [123]. Additionally, iodine-modified catechol was also demonstrated to be cytotoxic when directly contacting fibroblasts [37]. To improve the biocompatibility of halogenated catechol, a temporary and pH-responsive protecting group such as boronic acid could potentially be incorporated [124,125]. The utilization of ROS is an attractive antimicrobial strategy due to its short half-life and biocompatible degradation products (i.e., water and oxygen) [35]. ROS is also a natural disinfectant generated as part of normal wound healing response [79]. However, elevated levels of ROS can destroy healthy tissues, retard wound healing, and induce tumor formation [126,127]. Silica nanoparticles that catalyze the degradation of ROS could potentially be incorporated to modulate the concentration of the released ROS [128].

One of the often-overlooked issues in designing catechol-based coating is the long-term stability of the surface-bound catechol. There have only been limited studies that characterized the performance of these coatings in the presence of biomolecules or cells, or in vivo for 7 days or longer [129,130]. Catechol forms both reversible and irreversible interfacial bonds depending on the surface type [22–24], and it is potentially feasible for catechol to detach from inorganic surfaces over time. Recently, in situ electrochemical oxidation was found to deactivate and detach catechol-containing adhesive that was adhered to a titanium surface [131]. As such, externally applied force and oxidative stress can potentially lead to catechol delamination. While synthetic mussel adhesive mimics predominantly utilize catechol for adhesion, mussel adhesive proteins utilize a combination of different amino acid residues (i.e., charged, hydrophobic, etc.) and intermolecular chemical interactions between multiple proteins to create adhesive plaques that bind tightly to the substrate surface [23]. Incorporation of diverse interfacial chemistries may be necessary to strengthen coating stability. Additionally, there is a potentially need for strategies that preserve the reduced and adhesive form of catechol so that the delaminated catechol may reattach. The incorporation of an antioxidant thiol functional group [132], acidic side chain for buffering local solution pH [133], and temporary protecting groups such as boronic acid [134] can be used to prevent catechol oxidation.

**Author Contributions:** Conceptualization, B.L. and B.P.L.; writing—original draft preparation, S.R., K.W.; writing—review and editing, B.L. and B.P.L.; supervision, B.P.L. All authors have read and agreed to the published version of the manuscript.

**Funding:** The authors acknowledge funding from the National Institutes of Health under award no. R15GM135875 (B.P.L.), the Office of the Assistant Secretary of Defense for Health Affairs through the Defense Medical Research and Development Program under award No. W81XWH1810610 (B.P.L.), the Office of Naval Research under award No. N00014-20-1-2230 (B.P.L.), and the National Science Foundation under award No. DMR 2001076 (B.P.L.).

**Conflicts of Interest:** The authors declare no conflict of interest.

## References

1. Li, S.; Dong, S.; Xu, W.; Tu, S.; Yan, L.; Zhao, C.; Ding, J.; Chen, X. Antibacterial Hydrogels. *Adv. Sci.* **2018**, *5*, 1700527. [[CrossRef](#)] [[PubMed](#)]
2. Song, J.; Jang, J. Antimicrobial polymer nanostructures: Synthetic route, mechanism of action and perspective. *Adv. Colloid Interface Sci.* **2014**, *203*, 37–50. [[CrossRef](#)] [[PubMed](#)]
3. Baym, M.; Stone, L.K.; Kishony, R. Multidrug evolutionary strategies to reverse antibiotic resistance. *Science* **2016**, *351*, aad3292. [[CrossRef](#)] [[PubMed](#)]
4. Ren, W.; Cheng, W.; Wang, G.; Liu, Y. Developments in antimicrobial polymers. *J. Polym. Sci. Part. A Polym. Chem.* **2017**, *55*, 632–639. [[CrossRef](#)]
5. Muñoz-Bonilla, A.; Fernández-García, M. Polymeric materials with antimicrobial activity. *Prog. Polym. Sci.* **2012**, *37*, 281–339. [[CrossRef](#)]
6. Engler, A.C.; Wiradharma, N.; Ong, Z.Y.; Coady, D.J.; Hedrick, J.L.; Yang, Y.-Y. Emerging trends in macromolecular antimicrobials to fight multi-drug-resistant infections. *Nano Today* **2012**, *7*, 201–222. [[CrossRef](#)]

7. Jain, A.; Duvvuri, L.S.; Farah, S.; Beyth, N.; Domb, A.J.; Khan, W. Antimicrobial polymers. *Adv. Healthc Mater.* **2014**, *3*, 1969–1985. [[CrossRef](#)]
8. Kenawyel, R.; Worley, S.D.; Broughton, R. The chemistry and applications of antimicrobial polymers: A state-of-the-art review. *Biomacromolecules* **2007**, *8*, 1359–1384. [[CrossRef](#)]
9. Timofeeva, L.; Kleshcheva, N. Antimicrobial polymers: Mechanism of action, factors of activity, and applications. *Appl. Microbiol. Biotechnol.* **2011**, *89*, 475–492. [[CrossRef](#)]
10. Tew, G.N.; Scott, R.W.; Klein, M.L.; DeGrado, W.F. De Novo Design of Antimicrobial Polymers, Foldamers, and Small Molecules: From Discovery to Practical Applications. *Acc. Chem. Res.* **2010**, *43*, 30–39. [[CrossRef](#)]
11. Li, P.; Li, X.; Saravanan, R.; Li, C.M.; Leong, S.S.J. Antimicrobial macromolecules: Synthesis methods and future applications. *Rsc Adv.* **2012**, *2*, 4031–4044. [[CrossRef](#)]
12. Yang, Y.; Cai, Z.; Huang, Z.; Tang, X.; Zhang, X. Antimicrobial cationic polymers: From structural design to functional control. *Polym. J.* **2018**, *50*, 33–44. [[CrossRef](#)]
13. Carmona-Ribeiro, A.M.; de Melo Carrasco, L.D. Cationic antimicrobial polymers and their assemblies. *Int. J. Mol. Sci.* **2013**, *14*, 9906–9946. [[CrossRef](#)] [[PubMed](#)]
14. Santos, M.R.E.; Fonseca, A.C.; Mendonça, P.V.; Branco, R.; Serra, A.C.; Morais, P.V.; Coelho, J.F.J. Recent Developments in Antimicrobial Polymers: A Review. *Materials* **2016**, *9*, 599. [[CrossRef](#)] [[PubMed](#)]
15. Kamaruzzaman, N.F.; Tan, L.P.; Hamdan, R.H.; Choong, S.S.; Wong, W.K.; Gibson, A.J.; Chivu, A.; Pina, M.d.F. Antimicrobial Polymers: The Potential Replacement of Existing Antibiotics? *Int. J. Mol. Sci.* **2019**, *20*, 2747. [[CrossRef](#)]
16. Rotem, S.; Mor, A. Antimicrobial peptide mimics for improved therapeutic properties. *Biochim. Biophys. Acta Biomembr.* **2009**, *1788*, 1582–1592. [[CrossRef](#)]
17. Sobczak, M.; Dębek, C.; Ołędzka, E.; Kozłowski, R. Polymeric systems of antimicrobial peptides—strategies and potential applications. *Molecules* **2013**, *18*, 14122–14137. [[CrossRef](#)]
18. Huang, K.-S.; Yang, C.-H.; Huang, S.-L.; Chen, C.-Y.; Lu, Y.-Y.; Lin, Y.-S. Recent Advances in Antimicrobial Polymers: A Mini-Review. *Int. J. Mol. Sci.* **2016**, *17*, 1578. [[CrossRef](#)]
19. Sánchez-López, E.; Gomes, D.; Esteruelas, G.; Bonilla, L.; Lopez-Machado, A.L.; Galindo, R.; Cano, A.; Espina, M.; Ettcheto, M.; Camins, A.; et al. Metal-Based Nanoparticles as Antimicrobial Agents: An Overview. *Nanomaterials* **2020**, *10*, 292. [[CrossRef](#)]
20. Munoz-Bonilla, A.; Echeverria, C.; Sonseca, A.; Arrieta, M.P.; Fernandez-Garcia, M. Bio-Based Polymers with Antimicrobial Properties towards Sustainable Development. *Materials* **2019**, *12*, 641. [[CrossRef](#)]
21. Querido, M.M.; Aguiar, L.; Neves, P.; Pereira, C.C.; Teixeira, J.P. Self-disinfecting surfaces and infection control. *Colloids Surf. B Biointerfaces* **2019**, *178*, 8–21. [[CrossRef](#)] [[PubMed](#)]
22. Ahn, B.K. Perspectives on Mussel-Inspired Wet Adhesion. *J. Am. Chem. Soc.* **2017**, *139*, 10166–10171. [[CrossRef](#)] [[PubMed](#)]
23. Kord Forooshani, P.; Lee, B.P. Recent approaches in designing bioadhesive materials inspired by mussel adhesive protein. *J. Polym. Sci. Part. A Polym. Chem.* **2017**, *55*, 9–33. [[CrossRef](#)] [[PubMed](#)]
24. Lee, B.P.; Messersmith, P.B.; Israelachvili, J.N.; Waite, J.H. Mussel-Inspired Adhesives and Coatings. *Annu Rev. Mater. Res.* **2011**, *41*, 99–132. [[CrossRef](#)] [[PubMed](#)]
25. Waite, J.H.; Tanzer, M.L. Polyphenolic Substance of *Mytilus edulis*: Novel Adhesive Containing L-Dopa and Hydroxyproline. *Science* **1981**, *212*, 1038. [[CrossRef](#)]
26. Patil, N.; Jérôme, C.; Detrembleur, C. Recent advances in the synthesis of catechol-derived (bio)polymers for applications in energy storage and environment. *Prog. Polym. Sci.* **2018**, *82*, 34–91. [[CrossRef](#)]
27. Ye, Q.; Zhou, F.; Liu, W. Bioinspired catecholic chemistry for surface modification. *Chem. Soc. Rev.* **2011**, *40*, 4244–4258. [[CrossRef](#)]
28. Meng, H.; Forooshani, P.K.; Joshi, P.U.; Osborne, J.; Mi, X.; Meingast, C.; Pinnaratip, R.; Kelley, J.; Narkar, A.; He, W.; et al. Biomimetic recyclable microgels for on-demand generation of hydrogen peroxide and antipathogenic application. *Acta Biomater.* **2019**, *83*, 109–118. [[CrossRef](#)]
29. Kord Forooshani, P.; Polega, E.; Thomson, K.; Bhuiyan, M.S.A.; Pinnaratip, R.; Trought, M.; Kendrick, C.; Gao, Y.; Perrine, K.A.; Pan, L.; et al. Antibacterial Properties of Mussel-Inspired Polydopamine Coatings Prepared by a Simple Two-Step Shaking-Assisted Method. *Front. Chem.* **2019**, *7*. [[CrossRef](#)]
30. Zhang, W.; Wang, R.; Sun, Z.; Zhu, X.; Zhao, Q.; Zhang, T.; Cholewinski, A.; Yang, F.; Zhao, B.; Pinnaratip, R.; et al. Catechol-functionalized hydrogels: Biomimetic design, adhesion mechanism, and biomedical applications. *Chem. Soc. Rev.* **2020**, *49*, 433–464. [[CrossRef](#)]
31. Sileika, T.S.; Kim, H.-D.; Maniak, P.; Messersmith, P.B. Antibacterial Performance of Polydopamine-Modified Polymer Surfaces Containing Passive and Active Components. *ACS Appl. Mater. Interfaces* **2011**, *3*, 4602–4610. [[CrossRef](#)] [[PubMed](#)]
32. Wang, Z.; Zhao, S.; Song, R.; Zhang, W.; Zhang, S.; Li, J. The synergy between natural polyphenol-inspired catechol moieties and plant protein-derived bio-adhesive enhances the wet bonding strength. *Sci. Rep. UK* **2017**, *7*, 9664. [[CrossRef](#)] [[PubMed](#)]
33. Kim, K.; Shin, M.; Koh, M.-Y.; Ryu, J.H.; Lee, M.S.; Hong, S.; Lee, H. TAPE: A Medical Adhesive Inspired by a Ubiquitous Compound in Plants. *Adv. Funct. Mater.* **2015**, *25*, 2402–2410. [[CrossRef](#)]
34. Meng, H.; Li, Y.; Faust, M.; Konst, S.; Lee, B.P. Hydrogen peroxide generation and biocompatibility of hydrogel-bound mussel adhesive moiety. *Acta Biomater.* **2015**, *17*, 160–169. [[CrossRef](#)] [[PubMed](#)]
35. McDonnell, G. The Use of Hydrogen Peroxide for Disinfection and Sterilization Applications. In *PATAI'S Chemistry of Functional Groups*; John Wiley & Sons, Ltd.: Hoboken, NJ, USA, 2009. [[CrossRef](#)]

36. Dogan, E.M.; Sudur Zalluhoglu, F.; Orbey, N. Effect of potassium ion on the stability and release rate of hydrogen peroxide encapsulated in silica hydrogels. *Aiche J.* **2016**, *63*, 409–417. [[CrossRef](#)]
37. Liu, B.; Zhou, C.; Zhang, Z.; Roland, J.D.; Lee, B.P. Antimicrobial property of halogenated catechols. *Chem. Eng. J.* **2021**, *403*, 126340. [[CrossRef](#)]
38. Bouarab-Chibane, L.; Forquet, V.; Lantéri, P.; Clément, Y.; Léonard-Akkari, L.; Oulahal, N.; Degraeve, P.; Bordes, C. Antibacterial properties of polyphenols: Characterization and QSAR (Quantitative structure–activity relationship) models. *Front. Microbiol.* **2019**, *10*, 829. [[CrossRef](#)]
39. Daglia, M. Polyphenols as antimicrobial agents. *Curr. Opin. Biotechnol.* **2012**, *23*, 174–181. [[CrossRef](#)]
40. Choi, Y.-S.; Kang, H.; Kim, D.-G.; Cha, S.-H.; Lee, J.-C. Mussel-Inspired Dopamine- and Plant-Based Cardanol-Containing Polymer Coatings for Multifunctional Filtration Membranes. *ACS Appl. Mater. Interfaces* **2014**, *6*, 21297–21307. [[CrossRef](#)]
41. Faure, E.; Falentin-Daudré, C.; Jérôme, C.; Lyskawa, J.; Fournier, D.; Woisel, P.; Detrembleur, C. Catechols as versatile platforms in polymer chemistry. *Prog. Polym. Sci.* **2013**, *38*, 236–270. [[CrossRef](#)]
42. Himejima, M.; Kubo, I. Antibacterial agents from the cashew *Anacardium occidentale* (Anacardiaceae) nut shell oil. *J. Agric. Food Chem.* **1991**, *39*, 418–421. [[CrossRef](#)]
43. Choi, Y.-S.; Kim, K.-H.; Kim, D.-G.; Kim, H.J.; Cha, S.-H.; Lee, J.-C. Synthesis and characterization of self-cross-linkable and bactericidal methacrylate polymers having renewable cardanol moieties for surface coating applications. *RSC Adv.* **2014**, *4*, 41195–41203. [[CrossRef](#)]
44. Granger, R.E.; Campbell, E.L.; Johnston, G.A. (+)- And (-)-borneol: Efficacious positive modulators of GABA action at human recombinant  $\alpha 1\beta 2\gamma 2L$  GABA(A) receptors. *Biochem Pharm.* **2005**, *69*, 1101–1111. [[CrossRef](#)] [[PubMed](#)]
45. Luo, L.; Li, G.; Luan, D.; Yuan, Q.; Wei, Y.; Wang, X. Antibacterial Adhesion of Borneol-Based Polymer via Surface Chiral Stereochemistry. *ACS Appl. Mater. Interfaces* **2014**, *6*, 19371–19377. [[CrossRef](#)] [[PubMed](#)]
46. He, M.; Jiang, H.; Wang, R.; Xie, Y.; Zhao, W.; Zhao, C. A versatile approach towards multi-functional surfaces via covalently attaching hydrogel thin layers. *J. Colloid Interface Sci.* **2016**, *484*, 60–69. [[CrossRef](#)]
47. Wang, X.; Jing, S.; Liu, Y.; Liu, S.; Tan, Y. Diblock copolymer containing bioinspired borneol and dopamine moieties: Synthesis and antibacterial coating applications. *Polymer* **2017**, *116*, 314–323. [[CrossRef](#)]
48. Li, L.; Yan, B.; Yang, J.; Huang, W.; Chen, L.; Zeng, H. Injectable Self-Healing Hydrogel with Antimicrobial and Antifouling Properties. *ACS Appl. Mater. Interfaces* **2017**, *9*, 9221–9225. [[CrossRef](#)]
49. Plachá, D.; Muñoz-Bonilla, A.; Škrlová, K.; Echeverría, C.; Chiloeches, A.; Petr, M.; Lafdi, K.; Fernández-García, M. Antibacterial Character of Cationic Polymers Attached to Carbon-Based Nanomaterials. *Nanomaterials* **2020**, *10*, 1218. [[CrossRef](#)]
50. Han, H.; Wu, J.; Avery, C.W.; Mizutani, M.; Jiang, X.; Kamigaito, M.; Chen, Z.; Xi, C.; Kuroda, K. Immobilization of amphiphilic polycations by catechol functionality for antimicrobial coatings. *Langmuir ACS J. Surf. Colloids* **2011**, *27*, 4010–4019. [[CrossRef](#)]
51. Qiu, W.-Z.; Zhao, Z.-S.; Du, Y.; Hu, M.-X.; Xu, Z.-K. Antimicrobial membrane surfaces via efficient polyethyleneimine immobilization and cationization. *Appl. Surf. Sci.* **2017**, *426*, 972–979. [[CrossRef](#)]
52. Lemire, J.A.; Harrison, J.J.; Turner, R.J. Antimicrobial activity of metals: Mechanisms, molecular targets and applications. *Nat. Rev. Microbiol.* **2013**, *11*, 371–384. [[CrossRef](#)] [[PubMed](#)]
53. Dizaj, S.M.; Lotfipour, F.; Barzegar-Jalali, M.; Zarrintan, M.H.; Adibkia, K. Antimicrobial activity of the metals and metal oxide nanoparticles. *Mater. Sci. Eng. C* **2014**, *44*, 278–284. [[CrossRef](#)]
54. Xu, Z. Mechanics of metal-catecholate complexes: The roles of coordination state and metal types. *Sci. Rep.* **2013**, *3*, 2914. [[CrossRef](#)] [[PubMed](#)]
55. Andersen, A.; Chen, Y.; Birkedal, H. Bioinspired metal–polyphenol materials: Self-healing and beyond. *Biomimetics* **2019**, *4*, 30. [[CrossRef](#)] [[PubMed](#)]
56. Chen, J.; Peng, H.; Wang, X.; Shao, F.; Yuan, Z.; Han, H. Graphene oxide exhibits broad-spectrum antimicrobial activity against bacterial phytopathogens and fungal conidia by intertwining and membrane perturbation. *Nanoscale* **2014**, *6*, 1879–1889. [[CrossRef](#)]
57. Zollfrank, C.; Gutbrod, K.; Wechsler, P.; Guggenbichler, J.P. Antimicrobial activity of transition metal acid MoO(3) prevents microbial growth on material surfaces. *Mater. Sci. Eng. C Mater. Biol. Appl.* **2012**, *32*, 47–54. [[CrossRef](#)]
58. Nguyen, H.N.; Nadres, E.T.; Alamani, B.G.; Rodrigues, D.F. Designing polymeric adhesives for antimicrobial materials: Poly(ethylene imine) polymer, graphene, graphene oxide and molybdenum trioxide—A biomimetic approach. *J. Mater. Chem. B* **2017**, *5*, 6616–6628. [[CrossRef](#)]
59. Dakal, T.C.; Kumar, A.; Majumdar, R.S.; Yadav, V. Mechanistic Basis of Antimicrobial Actions of Silver Nanoparticles. *Front. Microbiol.* **2016**, *7*, 1831. [[CrossRef](#)]
60. Sadoon, A.A.; Khadka, P.; Freeland, J.; Gundampati, R.K.; Manso, R.H.; Ruiz, M.; Krishnamurthi, V.R.; Thallapuranam, S.K.; Chen, J.; Wang, Y. Silver Ions Caused Faster Diffusive Dynamics of Histone-Like Nucleoid-Structuring Proteins in Live Bacteria. *Appl. Environ. Microbiol.* **2020**, *86*, e02479-19. [[CrossRef](#)]
61. Tan, M.; Choi, Y.; Kim, J.; Kim, J.-H.; Fromm, K.M. Polyaspartamide Functionalized Catechol-Based Hydrogels Embedded with Silver Nanoparticles for Antimicrobial Properties. *Polymers* **2018**, *10*, 1188. [[CrossRef](#)]
62. Huang, X.; Bao, X.; Liu, Y.; Wang, Z.; Hu, Q. Catechol-Functional Chitosan/Silver Nanoparticle Composite as a Highly Effective Antibacterial Agent with Species-Specific Mechanisms. *Sci. Rep.* **2017**, *7*, 1860. [[CrossRef](#)] [[PubMed](#)]

63. Wang, R.; Song, X.; Xiang, T.; Liu, Q.; Su, B.; Zhao, W.; Zhao, C. Mussel-inspired chitosan-polyurethane coatings for improving the antifouling and antibacterial properties of polyethersulfone membranes. *Carbohydr. Polym.* **2017**, *168*, 310–319. [[CrossRef](#)] [[PubMed](#)]
64. Cheng, Y.F.; Zhang, J.Y.; Wang, Y.B.; Li, C.M.; Lu, Z.S.; Hu, X.F.; Xu, L.Q. Deposition of catechol-functionalized chitosan and silver nanoparticles on biomedical titanium surfaces for antibacterial application. *Mater. Sci. Eng. C* **2019**, *98*, 649–656. [[CrossRef](#)] [[PubMed](#)]
65. Falentin-Daudré, C.; Faure, E.; Svaldo-Lanero, T.; Farina, F.; Jérôme, C.; Van De Weerd, C.; Martial, J.; Duwez, A.-S.; Detrembleur, C. Antibacterial Polyelectrolyte Micelles for Coating Stainless Steel. *Langmuir* **2012**, *28*, 7233–7241. [[CrossRef](#)] [[PubMed](#)]
66. Charlot, A.; Sciannaméa, V.; Lenoir, S.; Faure, E.; Jérôme, R.; Jérôme, C.; Van De Weerd, C.; Martial, J.; Archambeau, C.; Willet, N.; et al. All-in-one strategy for the fabrication of antimicrobial biomimetic films on stainless steel. *J. Mater. Chem.* **2009**, *19*, 4117–4125. [[CrossRef](#)]
67. Le Thi, P.; Lee, Y.; Hoang Thi, T.T.; Park, K.M.; Park, K.D. Catechol-rich gelatin hydrogels in situ hybridizations with silver nanoparticle for enhanced antibacterial activity. *Mater. Sci. Eng. C* **2018**, *92*, 52–60. [[CrossRef](#)]
68. GhavamiNejad, A.; Park, C.H.; Kim, C.S. In Situ Synthesis of Antimicrobial Silver Nanoparticles within Antifouling Zwitterionic Hydrogels by Catecholic Redox Chemistry for Wound Healing Application. *Biomacromolecules* **2016**, *17*, 1213–1223. [[CrossRef](#)]
69. Sambale, F.; Wagner, S.; Stahl, F.; Khaydarov, R.R.; Scheper, T.; Bahnemann, D. Investigations of the Toxic Effect of Silver Nanoparticles on Mammalian Cell Lines. *J. Nanomater.* **2015**, *2015*, 136765. [[CrossRef](#)]
70. AshaRani, P.V.; Low Kah Mun, G.; Hande, M.P.; Valiyaveetil, S. Cytotoxicity and Genotoxicity of Silver Nanoparticles in Human Cells. *ACS Nano* **2009**, *3*, 279–290. [[CrossRef](#)]
71. Nie, C.; Cheng, C.; Ma, L.; Deng, J.; Zhao, C. Mussel-Inspired Antibacterial and Biocompatible Silver–Carbon Nanotube Composites: Green and Universal Nanointerfacial Functionalization. *Langmuir* **2016**, *32*, 5955–5965. [[CrossRef](#)]
72. Gan, D.; Xing, W.; Jiang, L.; Fang, J.; Zhao, C.; Ren, F.; Fang, L.; Wang, K.; Lu, X. Plant-inspired adhesive and tough hydrogel based on Ag-Lignin nanoparticles-triggered dynamic redox catechol chemistry. *Nat. Commun.* **2019**, *10*, 1487. [[CrossRef](#)] [[PubMed](#)]
73. Harrington, M.J.; Masic, A.; Holten-Andersen, N.; Waite, J.H.; Fratzl, P. Iron-clad fibers: A metal-based biological strategy for hard flexible coatings. *Science* **2010**, *328*, 216–220. [[CrossRef](#)] [[PubMed](#)]
74. Kim, S.; Moon, J.-M.; Choi, J.S.; Cho, W.K.; Kang, S.M. Mussel-Inspired Approach to Constructing Robust Multilayered Alginate Films for Antibacterial Applications. *Adv. Funct. Mater.* **2016**, *26*, 4099–4105. [[CrossRef](#)]
75. Lee, H.; Dellatore, S.M.; Miller, W.M.; Messersmith, P.B. Mussel-inspired surface chemistry for multifunctional coatings. *Science* **2007**, *318*, 426–430. [[CrossRef](#)]
76. Ji, C.; Juárez-Hernández, R.E.; Miller, M.J. Exploiting bacterial iron acquisition: Siderophore conjugates. *Future Med. Chem.* **2012**, *4*, 297–313. [[CrossRef](#)] [[PubMed](#)]
77. Kinzel, O.; Tappe, R.; Gerus, I.; Budzikiewicz, H. The synthesis and antibacterial activity of two pyoverdinin-ampicillin conjugates, entering *Pseudomonas aeruginosa* via the pyoverdinin-mediated iron uptake pathway. *J. Antibiot.* **1998**, *51*, 499–507. [[CrossRef](#)]
78. Ohi, N.; Aoki, B.; Kuroki, T.; Matsumoto, M.; Kojima, K.; Nehashi, T. Semisynthetic beta-lactam antibiotics. III. Effect on antibacterial activity and comt-susceptibility of chlorine-introduction into the catechol nucleus of 6-[(R)-2-[3-(3,4-dihydroxybenzoyl)-3-(3-hydroxypropyl)-1-ureido]-2-phenylacetamido]penicillanic acid. *J. Antibiot.* **1987**, *40*, 22–28. [[CrossRef](#)]
79. Forooshani, P.K.; Meng, H.; Lee, B.P. Catechol Redox Reaction: Reactive Oxygen Species Generation, Regulation, and Biomedical Applications. In *Advances in Bioinspired and Biomedical Materials Volume 1*; American Chemical Society: Washington, DC, USA, 2017; Volume 1252, pp. 179–196.
80. Yagub, M.T.; Sen, T.K.; Afroze, S.; Ang, H.M. Dye and its removal from aqueous solution by adsorption: A review. *Adv. Colloid Interface Sci.* **2014**, *209*, 172–184. [[CrossRef](#)]
81. Fu, F.; Wang, Q. Removal of heavy metal ions from wastewaters: A review. *J. Environ. Manag.* **2011**, *92*, 407–418. [[CrossRef](#)]
82. Gothwal, R.; Shashidhar, T. Antibiotic Pollution in the Environment: A Review. *Clean Soil Air Water* **2015**, *43*, 479–489. [[CrossRef](#)]
83. Ye, Y.; Xiao, L.; Bin, H.; Zhang, Q.; Nie, T.; Yang, X.; Wu, D.; Cheng, H.; Li, P.; Wang, Q. Oxygen-tuned nanozyme polymerization for the preparation of hydrogels with printable and antibacterial properties. *J. Mater. Chem. B* **2017**, *5*, 1518–1524. [[CrossRef](#)] [[PubMed](#)]
84. Fridovich, I. The biology of oxygen radicals. *Science* **1978**, *201*, 875–880. [[CrossRef](#)] [[PubMed](#)]
85. Ghosh, N.; Das, A.; Chaffee, S.; Roy, S.; Sen, C.K. Chapter 4—Reactive Oxygen Species, Oxidative Damage and Cell Death. In *Immunity and Inflammation in Health and Disease*; Chatterjee, S., Jungraithmayr, W., Bagchi, D., Eds.; Academic Press: Cambridge, MA, USA, 2018. [[CrossRef](#)]
86. Fang, F.C. Antimicrobial Actions of Reactive Oxygen Species. *mBio* **2011**, *2*, e00141-11. [[CrossRef](#)] [[PubMed](#)]
87. Kalyanaraman, B.; Felix, C.C.; Sealy, R.C. Semiquinone anion radicals of catechol(amine)s, catechol estrogens, and their metal ion complexes. *Environ. Health Perspect.* **1985**, *64*, 185–198. [[CrossRef](#)]
88. Zhang, Z.; He, X.; Zhou, C.; Reaume, M.; Wu, M.; Liu, B.; Lee, B.P. Iron Magnetic Nanoparticle-Induced ROS Generation from Catechol-Containing Microgel for Environmental and Biomedical Applications. *ACS Appl. Mater. Interfaces* **2020**, *12*, 21210–21220. [[CrossRef](#)]
89. Mustafa, H.S.I. Staphylococcus aureus Can Produce Catalase Enzyme When Adding to Human WBCs as a Source of H<sub>2</sub>O<sub>2</sub> Productions in Human Plasma or Serum in the Laboratory. *Open J. Med. Microbiol.* **2014**, *4*, 249. [[CrossRef](#)]

90. Kord Forooshani, P.; Pinnaratip, R.; Polega, E.; Tyo, A.G.; Pearson, E.; Liu, B.; Folayan, T.-O.; Pan, L.; Rajachar, R.M.; Heldt, C.L.; et al. Hydroxyl Radical Generation through the Fenton-like Reaction of Hematin- and Catechol-Functionalized Microgels. *Chem. Mater.* **2020**. [[CrossRef](#)]
91. Buxton, G.V.; Greenstock, C.L.; Helman, W.P.; Ross, A.B. Critical Review of rate constants for reactions of hydrated electrons, hydrogen atoms and hydroxyl radicals (OH/O<sup>-</sup> in Aqueous Solution. *J. Phys. Chem. Ref. Data* **1988**, *17*, 513–886. [[CrossRef](#)]
92. Sies, H. Strategies of antioxidant defense. *EJB Rev.* **1994**, *1993*, 101–107.
93. Kruk, I.; Lichszteid, K.; Michalska, T.; Wronska, J.; Bounias, M. The Formation of Singlet Oxygen during Oxidation of Catechol Amines as Detected by Infrared Chemiluminescence and Spectrophotometric Method. *Z. Nat. C* **1989**, *44*, 895–900. [[CrossRef](#)]
94. Tyo, A.; Welch, S.; Hennenfent, M.; Kord Fooroshani, P.; Lee, B.P.; Rajachar, R. Development and Characterization of an Antimicrobial Polydopamine Coating for Conservation of Humpback Whales. *Front. Chem.* **2019**. [[CrossRef](#)] [[PubMed](#)]
95. Lucchini, J.; Corre, J.; Cremieux, A. Antibacterial activity of phenolic compounds and aromatic alcohols. *Res. Microbiol.* **1990**, *141*, 499–510. [[CrossRef](#)]
96. Sivaraman, S.; Sullivan, T.J.; Johnson, F.; Novichenok, P.; Cui, G.; Simmerling, C.; Tonge, P.J. Inhibition of the bacterial enoyl reductase FabI by triclosan: A structure– reactivity analysis of FabI inhibition by triclosan analogues. *J. Med. Chem.* **2004**, *47*, 509–518. [[CrossRef](#)] [[PubMed](#)]
97. Rafi, S.B.; Cui, G.; Song, K.; Cheng, X.; Tonge, P.J.; Simmerling, C. Insight through molecular mechanics Poisson– Boltzmann surface area calculations into the binding affinity of triclosan and three analogues for FabI, the *E. coli* enoyl reductase. *J. Med. Chem.* **2006**, *49*, 4574–4580. [[CrossRef](#)] [[PubMed](#)]
98. Sun, C.J.; Srivastava, A.; Reifert, J.R.; Waite, J.H. Halogenated DOPA in a marine adhesive protein. *J. Adhes.* **2009**, *85*, 126–138. [[CrossRef](#)] [[PubMed](#)]
99. García-Fernández, L.; Cui, J.; Serrano, C.; Shafiq, Z.; Gropeanu, R.A.; Miguel, V.S.; Ramos, J.I.; Wang, M.; Auernhammer, G.K.; Ritz, S. Antibacterial Strategies from the Sea: Polymer-Bound Cl-Catechols for Prevention of Biofilm Formation. *Adv. Mater.* **2013**, *25*, 529–533. [[CrossRef](#)]
100. Chien, H.-W.; Chiu, T.-H. Stable N-halamine on polydopamine coating for high antimicrobial efficiency. *Eur. Polym. J.* **2020**, *130*, 109654. [[CrossRef](#)]
101. Widsten, P.; Heathcote, C.; Kandelbauer, A.; Guebitz, G.; Nyanhongo, G.S.; Prasetyo, E.N.; Kudanga, T. Enzymatic surface functionalisation of lignocellulosic materials with tannins for enhancing antibacterial properties. *Process. Biochem.* **2010**, *45*, 1072–1081. [[CrossRef](#)]
102. Scalbert, A. Antimicrobial properties of tannins. *Phytochemistry* **1991**, *30*, 3875–3883. [[CrossRef](#)]
103. Sahiner, N.; Sagbas, S.; Sahiner, M.; Silan, C.; Aktas, N.; Turk, M. Biocompatible and biodegradable poly (Tannic Acid) hydrogel with antimicrobial and antioxidant properties. *Int. J. Biol. Macromol.* **2016**, *82*, 150–159. [[CrossRef](#)]
104. Li, N.; Yang, X.; Liu, W.; Xi, G.; Wang, M.; Liang, B.; Ma, Z.; Feng, Y.; Chen, H.; Shi, C. Tannic acid cross-linked polysaccharide-based multifunctional hemostatic microparticles for the regulation of rapid wound healing. *Macromol. Biosci.* **2018**, *18*, 1800209. [[CrossRef](#)] [[PubMed](#)]
105. Liu, R.; Zheng, J.; Guo, R.; Luo, J.; Yuan, Y.; Liu, X. Synthesis of New Biobased Antibacterial Methacrylates Derived from Tannic Acid and Their Application in UV-Cured Coatings. *Ind. Eng. Chem. Res.* **2014**, *53*, 10835–10840. [[CrossRef](#)]
106. Mori, A.; Nishino, C.; Enoki, N.; Tawata, S. Antibacterial activity and mode of action of plant flavonoids against *Proteus vulgaris* and *Staphylococcus aureus*. *Phytochemistry* **1987**, *26*, 2231–2234. [[CrossRef](#)]
107. Nguyen, T.T.T.; Ghosh, C.; Hwang, S.-G.; Dai Tran, L.; Park, J.S. Characteristics of curcumin-loaded poly (lactic acid) nanofibers for wound healing. *J. Mater. Sci.* **2013**, *48*, 7125–7133. [[CrossRef](#)]
108. Xie, M.; Fan, D.; Zhao, Z.; Li, Z.; Li, G.; Chen, Y.; He, X.; Chen, A.; Li, J.; Lin, X. Nano-curcumin prepared via supercritical: Improved anti-bacterial, anti-oxidant and anti-cancer efficacy. *Int. J. Pharm.* **2015**, *496*, 732–740. [[CrossRef](#)]
109. Murase, T.; Nagasawa, A.; Suzuki, J.; Hase, T.; Tokimitsu, I. Beneficial effects of tea catechins on diet-induced obesity: Stimulation of lipid catabolism in the liver. *Int. J. Obes.* **2002**, *26*, 1459–1464. [[CrossRef](#)] [[PubMed](#)]
110. Sakihama, Y.; Cohen, M.F.; Grace, S.C.; Yamasaki, H. Plant phenolic antioxidant and prooxidant activities: Phenolics-induced oxidative damage mediated by metals in plants. *Toxicology* **2002**, *177*, 67–80. [[CrossRef](#)]
111. Awan, J.A.; Rehman, S.U.; Kashif Bangash, M.; Hussain, F.; Jaubert, J.-N. Development and characterization of electrospun curcumin-loaded antimicrobial nanofibrous membranes. *Text. Res. J.* **2020**. [[CrossRef](#)]
112. Ana, T.; Nieves, B.; Raul, D.; Ana, B.; Eduardo, R.; Diego, M.; Cristina, G. Natural bioactive compounds from winery by-products as health promoters. *Int. J. Mol. Sci.* **2014**, *15*, 15638–15678.
113. Sato, J.; Nakayama, M.; Tomita, A.; Sonoda, T.; Miyamoto, T. Difference in the antibacterial action of epigallocatechin gallate and theaflavin 3, 3'-di-O-gallate on *Bacillus coagulans*. *J. Appl. Microbiol.* **2020**, *129*, 601–611. [[CrossRef](#)]
114. George, D.; Begum, K.M.S.; Maheswari, P.U. Sugarcane bagasse (SCB) based pristine cellulose hydrogel for delivery of grape pomace polyphenol drug. *Waste Biomass Valorization* **2020**, *11*, 851–860. [[CrossRef](#)]
115. Guo, L.; Yang, Z.-Y.; Tang, R.-C.; Yuan, H.-B. Grape Seed Proanthocyanidins: Novel Coloring, Flame-Retardant, and Antibacterial Agents for Silk. *ACS Sustain. Chem. Eng.* **2020**, *8*, 5966–5974. [[CrossRef](#)]
116. Li, Y.; Meng, H.; Liu, Y.; Narkar, A.; Lee, B.P. Gelatin Microgel Incorporated Poly(ethylene glycol)-Based Bioadhesive with Enhanced Adhesive Property and Bioactivity. *ACS Appl. Mater. Interfaces* **2016**, *8*, 11980–11989. [[CrossRef](#)] [[PubMed](#)]



117. Liu, Y.; Meng, H.; Konst, S.; Sarmiento, R.; Rajachar, R.; Lee, B.P. Injectable Dopamine-Modified Poly(Ethylene Glycol) Nanocomposite Hydrogel with Enhanced Adhesive Property and Bioactivity. *ACS Appl. Mater. Interfaces* **2014**, *6*, 16982–16992. [[CrossRef](#)]
118. Mehdizadeh, M.; Weng, H.; Gyawali, D.; Tang, L.; Yang, J. Injectable citrate-based mussel-inspired tissue bioadhesives with high wet strength for sutureless wound closure. *Biomaterials* **2012**, *33*, 7972–7983. [[CrossRef](#)]
119. Brubaker, C.E.; Kissler, H.; Wang, L.-J.; Kaufman, D.B.; Messersmith, P.B. Biological performance of mussel-inspired adhesive in extrahepatic islet transplantation. *Biomaterials* **2010**, *31*, 420–427. [[CrossRef](#)]
120. Colinas, I.R.; Rojas-Andrade, M.D.; Chakraborty, I.; Oliver, S.R. Two structurally diverse Zn-based coordination polymers with excellent antibacterial activity. *Cryst. Eng. Comm.* **2018**, *20*, 3353–3362. [[CrossRef](#)]
121. Patel, K.M.; Patel, K.; Patel, N.; Patel, M. Synthesis, characterization, and antimicrobial activities of some transition metal complexes with a tridentate dibasic Schiff base and bidentate 2, 2'-bipyridylamine. *Synth. React. Inorg. Met. Org. Chem.* **2001**, *31*, 239–246. [[CrossRef](#)]
122. Huppmann, T.; Yatsenko, S.; Leonhardt, S.; Krampe, E.; Radovanovic, I.; Bastian, M.; Wintermantel, E. Antimicrobial polymers—The Antibacterial Effect of Photoactivated Nano Titanium Dioxide Polymer Composites. In *AIP Conference Proceedings*; American Institute of Physics: University Park City, MD, USA, 2014; pp. 440–443.
123. Neilson, A.H.; Allard, A.S.; Hynning, P.Å.; Remberger, M. Distribution, fate and persistence of organochlorine compounds formed during production of bleached pulp. *Toxicol. Environ. Chem.* **1991**, *30*, 3–41. [[CrossRef](#)]
124. Pizer, R.; Babcock, L. Mechanism of the complexation of boron acids with catechol and substituted catechols. *Inorg. Chem.* **1977**, *16*, 1677–1681. [[CrossRef](#)]
125. Wang, G.; Chen, X.; Liu, S.; Wong, C.; Chu, S. Mechanical chameleon through dynamic real-time plasmonic tuning. *ACS Nano* **2016**, *10*, 1788–1794. [[CrossRef](#)] [[PubMed](#)]
126. Loo, A.E.K.; Wong, Y.T.; Ho, R.; Wasser, M.; Du, T.; Ng, W.T.; Halliwell, B. Effects of Hydrogen Peroxide on Wound Healing in Mice in Relation to Oxidative Damage. *PLoS ONE* **2012**, *7*, e49215. [[CrossRef](#)] [[PubMed](#)]
127. Brian, N.; Ahswin, H.; Smart, N.; Bayon, Y.; Wohlert, S.; Hunt, J.A. Reactive Oxygen Species (ROS)—A Family of Fate Deciding Molecules Pivotal in Constructive Inflammation and Wound Healing. *Eur. Cells Mater.* **2012**, *24*, 249–265. [[CrossRef](#)]
128. Pinnaratip, R.; Forooshani, P.K.; Li, M.; Hu, Y.H.; Rajachar, R.M.; Lee, B.P. Controlling the Release of Hydrogen Peroxide from Catechol-Based Adhesives Using Silica Nanoparticles. *ACS Biomater. Sci. Eng.* **2020**, *6*, 4502–4511. [[CrossRef](#)] [[PubMed](#)]
129. Statz, A.R.; Barron, A.E.; Messersmith, P.B. Protein, cell and bacterial fouling resistance of polypeptoid-modified surfaces: Effect of side-chain chemistry. *Soft Matter* **2008**, *4*, 131–139. [[CrossRef](#)]
130. Pechey, A.; Elwood, C.N.; Wignall, G.R.; Dalsin, J.L.; Lee, B.P.; Vanjcek, M.; Welch, I.; Ko, R.; Razvi, H.; Cadieux, P.A. Anti-adhesive coating and clearance of device associated uropathogenic escherichia coli cystitis. *J. Urol.* **2009**, *182*, 1628–1636. [[CrossRef](#)]
131. Bhuiyan, M.S.A.; Roland, J.D.; Liu, B.; Reaume, M.; Zhang, Z.; Kelley, J.D.; Lee, B.P. In Situ Deactivation of Catechol-Containing Adhesive Using Electrochemistry. *J. Am. Chem. Soc.* **2020**, *142*, 4631–4638. [[CrossRef](#)]
132. Nicklisch, S.C.; Spahn, J.E.; Zhou, H.; Gruian, C.M.; Waite, J.H. Redox Capacity of an Extracellular Matrix Protein Associated with Adhesion in *Mytilus californianus*. *Biochemistry* **2016**, *55*, 2022–2030. [[CrossRef](#)]
133. Narkar, A.R.; Kelley, J.D.; Pinnaratip, R.; Lee, B.P. Effect of Ionic Functional Groups on the Oxidation State and Interfacial Binding Property of Catechol-Based Adhesive. *Biomacromolecules* **2018**, *19*, 1416–1424. [[CrossRef](#)]
134. Narkar, A.R.; Barker, B.; Clisch, M.; Jiang, J.; Lee, B.P. pH Responsive and Oxidation Resistant Wet Adhesive based on Reversible Catechol–Boronate Complexation. *Chem. Mater.* **2016**, *28*, 5432–5439. [[CrossRef](#)]